

# Neutrino Masses from $\mathcal{Z}_8$ Scoto-Seesaw Model with Spontaneous CP Violation

D. M. Barreiros,<sup>†1</sup> F. R. Joaquim,<sup>1</sup> R. Srivastava,<sup>2</sup> and J. W. F. Valle<sup>3</sup>

<sup>1</sup>*Departamento de Física and CFTP, Instituto Superior Técnico, Universidade de Lisboa, Av. Rovisco Pais, 1, 1049-001 Lisboa, Portugal*

<sup>2</sup>*Department of Physics, Indian Institute of Science Education and Research - Bhopal, Bhopal Bypass Road, Bhauri, Bhopal, India*

<sup>3</sup>*AHEP Group, Institut de Física Corpuscular – C.S.I.C./Universitat de València, Parc Científic de Paterna. C/ Catedrático José Beltrán, 2 E-46980 Paterna (Valencia), Spain*

## Abstract

We consider a scoto-seesaw model where dark matter, neutrino masses and spontaneous CP violation are accommodated using a single horizontal  $\mathcal{Z}_8$  symmetry. This symmetry is broken down to a dark  $\mathcal{Z}_2$  by the complex vacuum expectation value of a scalar singlet, stabilizing dark matter and providing a spontaneous origin for leptonic CP violation. We conclude that the imposed  $\mathcal{Z}_8$  symmetry constrains the lightest neutrino mass and the Dirac phase to intervals currently probed by experiments. For a normally-ordered neutrino mass spectrum, the allowed compatibility regions will soon be fully scrutinized by neutrinoless double beta decay experiments and cosmological observations.\*

*Keywords:* neutrino physics, CP violation

*DOI:* 10.31526/ACP.BSM-2021.32

## 1. INTRODUCTION

A new chapter in the field of particle physics was opened when neutrino oscillation experiments established the existence of neutrino masses. The need to go beyond the Standard Model (SM) is, thus, well motivated not only as a way of finding models that attempt at explaining the origin of neutrino masses, but also to unveil several other open questions like the understanding and interpretation of cosmological dark matter (DM), or finding symmetries responsible for the observed lepton mixing pattern. In fact, using DM as a mediator for neutrino mass generation [2] is a very attractive idea [3, 4, 5, 6, 7, 8, 9, 10, 11, 12, 13, 14, 15, 16, 17, 18] and complements the seesaw mechanism by giving a central role to DM. This scheme may also allow for CP violation and give insightful information about the lepton flavour structure seen in neutrino oscillation data [19].

The simplest (3,1) version of the seesaw mechanism and the minimal scotogenic approach to DM have been previously combined in Ref. [20]. In that work, a two-scale framework for neutrino mass generation was obtained, in which the atmospheric scale has a type-I seesaw origin, while the solar scale arises at the radiative level through a scotogenic loop. Even though this simple model can accommodate neutrino oscillation and lepton flavour violation data, it does not provide any constraints on low-energy observables. In the present work, we are interested in adopting a minimal approach, where only one Abelian symmetry is used to constrain lepton mixing, assure DM stability and allow for spontaneous CP violation (SCPV).

We enlarge the minimal scoto-seesaw model of Ref. [20] with an extra right-handed neutrino, in a (3,2) scheme [21], and a new complex scalar singlet, as well as a simple Abelian symmetry, in order to address the neutrino oscillation flavour structure and implement a spontaneous origin for leptonic CP violation. The implemented symmetry plays an important role in stabilizing DM.

The layout of this paper is as follows. In Section 2, we present the minimal scheme required to implement the above-mentioned features of the model. The low-energy constraints that arise from our  $\mathcal{Z}_8$  symmetric model and their compatibility with neutrino oscillation and neutrinoless double beta decay data are discussed in Sections 3 and 4, respectively. Finally, in Section 5, we summarise our results and present our concluding remarks.

## 2. NEUTRINO MASSES, SPONTANEOUS CP VIOLATION AND DARK MATTER STABILITY IN THE SCOTO-SEESAW MECHANISM

In the context of the minimal scoto-seesaw model [20], the atmospheric and solar neutrino mass scales, measured in oscillation experiments, arise at tree level, via the type-I seesaw mechanism, and at loop level, via the scotogenic mechanism, respectively (see Fig. 1). The SM particle content is extended with one right-handed (RH) neutrino  $\nu_R$ , a new fermion singlet  $f$  and an extra scalar doublet  $\eta$ . The latter two particles are odd under a dark  $\mathcal{Z}_2$  symmetry which guarantees DM stability. With this field content, the lepton Yukawa and mass Lagrangian is given by

<sup>†</sup>Speaker

\*This contribution is based on the work of Ref. [1].

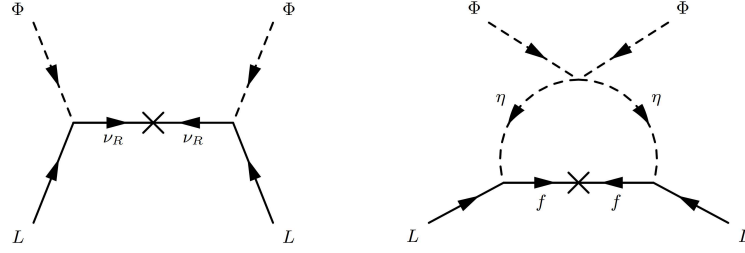


FIGURE 1: Neutrino mass generation contributions in the minimal scoto-seesaw model. The diagram on the left (right) shows the tree-level seesaw (one-loop scotogenic) realisations of the neutrino mass effective operator  $LL\Phi\Phi$ .

$$-\mathcal{L} = \bar{L}\mathbf{Y}_\ell\Phi e_R + \bar{L}\mathbf{Y}_\nu\tilde{\Phi}\nu_R + \frac{1}{2}M_R\bar{\nu}_R\nu_R^c + \bar{L}\mathbf{Y}_f^*\tilde{\eta}f + \frac{1}{2}M_f\bar{f}f^c + \text{H.c.} \quad (2.1)$$

Here,  $L = (\nu \ell)^T$  are left-handed (LH) lepton doublets,  $e_R$  are RH charged-lepton singlets,  $\Phi = (\phi^+ \phi^0)^T$  and  $\eta = (\eta^+ \eta^0)^T$  are both  $SU(2)_L$  doublets with  $\tilde{\Phi} = i\sigma_2\Phi^*$  and  $\tilde{\eta} = i\sigma_2\eta^*$ .  $\mathbf{Y}_\nu$  and  $\mathbf{Y}_f$  are general complex  $3 \times 1$  Yukawa coupling matrices, while  $M_{f,R}$  are the  $f$  and  $\nu_R$  masses. The effective neutrino mass matrix, generated after electroweak symmetry breaking, reads [20]

$$\mathbf{M}_\nu = -v^2 \frac{\mathbf{Y}_\nu \mathbf{Y}_\nu^T}{M_R} + \mathcal{F}(M_f, m_{\eta_R}, m_{\eta_I}) M_f \mathbf{Y}_f \mathbf{Y}_f^T, \quad (2.2)$$

where the first term accounts for the seesaw contribution and the second one gives the scotogenic loop correction. The loop factor  $\mathcal{F}$  is given by

$$\mathcal{F}(M_f, m_{\eta_R}, m_{\eta_I}) = \frac{1}{32\pi^2} \left[ \frac{m_{\eta_R}^2 \log\left(\frac{M_f^2}{m_{\eta_R}^2}\right)}{M_f^2 - m_{\eta_R}^2} - \frac{m_{\eta_I}^2 \log\left(\frac{M_f^2}{m_{\eta_I}^2}\right)}{M_f^2 - m_{\eta_I}^2} \right], \quad (2.3)$$

being  $m_{\eta_R}$  ( $m_{\eta_I}$ ) the mass of the real (imaginary) part of  $\eta = \eta_R + i\eta_I$ . Without any further consideration, this model accommodates neutrino data and fixes the lightest neutrino mass to zero. No other restrictions to oscillation parameters can be established.

A consequence of requiring the Lagrangian of Eq. (2.1) to be CP invariant is that all couplings and masses become real, leading to the absence of leptonic CP violation (LCPV). However, if we want to take advantage of the reduced number of parameters of the CP invariant model and, at the same time, have non-zero LCPV, then an alternative source of CP violation must be found. This can be done by adding a new complex scalar singlet  $\sigma$  to the scoto-seesaw model. This field acquires a complex vacuum expectation value (VEV)  $\langle\sigma\rangle = u e^{i\theta}$  that will possibly lead to LCPV through the couplings of  $\sigma/\sigma^*$  with  $f$  and  $\nu_R$  [22, 23]. If  $\sigma$  is even under the dark  $\mathcal{Z}_2$  symmetry, then the following couplings are allowed

$$\frac{1}{2}(y_R\sigma + \tilde{y}_R\sigma^*)\bar{\nu}_R\nu_R^c + \frac{1}{2}(y_f\sigma + \tilde{y}_f\sigma^*)\bar{f}f^c + \text{H.c.} \quad (2.4)$$

The contribution of the above terms to neutrino mass generation at tree and loop level is depicted in the diagrams of Fig. 2. Once  $\sigma$  acquires its VEV, the terms in Eq. (2.4) will contribute to effective neutrino mass matrix as

$$\mathbf{M}_\nu = -v^2 e^{i(\theta_f - \theta_R)} \frac{\mathbf{Y}_\nu \mathbf{Y}_\nu^T}{|M_R|} + \mathcal{F}(|M_f|, m_{\eta_R}, m_{\eta_I}) |M_f| \mathbf{Y}_f \mathbf{Y}_f^T, \quad (2.5)$$

where the  $\nu_R$  and  $f$  masses in Eq. (2.1) are written as  $M_{R,f} = |M_{R,f}| e^{i\theta_{R,f}}$  with,

$$|M_{R,f}|^2 = [y_{R,f}^2 + \tilde{y}_{R,f}^2 + 2y_{R,f}\tilde{y}_{R,f}\cos(2\theta_{R,f})] u^2, \quad (2.6)$$

and

$$\tan(\theta_f - \theta_R) = \frac{(y_f\tilde{y}_R - y_R\tilde{y}_f)\sin(2\theta)}{y_R y_f + \tilde{y}_R \tilde{y}_f + (y_R \tilde{y}_f + y_f \tilde{y}_R)\cos(2\theta)}. \quad (2.7)$$

The above equation shows that  $\theta_f - \theta_R$  is non-zero as long as one can guarantee that  $\theta \neq k\pi$  ( $k = 1, 2, \dots$ ) and  $y_{R,f} \neq \tilde{y}_{R,f}$ . In that case, CP violation will be successfully transmitted to the lepton sector. Also, from the diagrams of Fig. 2, it can be seen that the presence of CP violation in the effective neutrino masses matrix demands for a relative phase between the coefficients of the dimension-6 operators  $LL\Phi\Phi\sigma^*$  and  $LL\Phi\Phi\sigma$ .

In spite of being CP invariant at the Lagrangian level, the model with one single copy of  $\nu_R$  and  $f$  fermions, still has nine free parameters (six real Yukawa couplings, the  $\nu_R$  and  $f$  masses and the phase  $\theta_R - \theta_f$ ) to compare with the seven effective neutrino

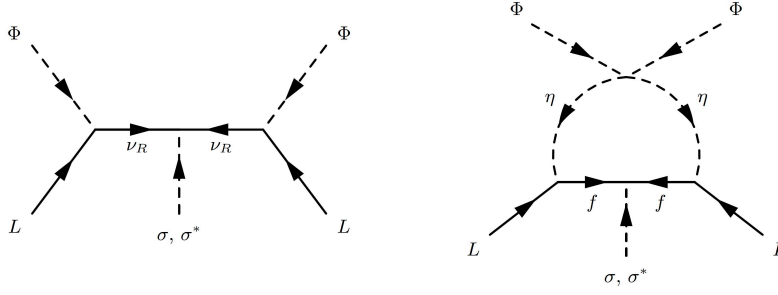


FIGURE 2: Neutrino mass generation contributions in the minimal scoto-seesaw model where LCPV is achieved through  $\nu_R$  and  $f$  couplings to a new complex scalar singlet  $\sigma$  and its complex conjugate  $\sigma^*$ .

parameters. As a matter of fact, if one tries to forbid some Yukawa couplings by using an Abelian flavour symmetry, one will always face incompatibility with neutrino oscillation data, due to the arising of either vanishing mixing angles or an extra massless neutrino. In order to solve this problem, we enlarge the minimal scoto-seesaw model with another  $\nu_R$  in the fermion sector. This allows to implement a horizontal flavour symmetry which then breaks to the dark  $\mathcal{Z}_2$  symmetry, ensuring DM stability.

In this extension to the scoto-seesaw model, the mass and lepton Yukawa Lagrangian corresponds to the one given in Eq. (2.1) with the difference that  $\nu_R$  is replaced by  $(\nu_{1R} \nu_{2R})^T$ , the mass  $M_R$  is now a  $2 \times 2$  matrix, and  $\mathbf{Y}_\nu$  becomes a  $3 \times 2$  matrix. The most restrictive patterns for the mass and Yukawa matrices which are compatible with neutrino data are given by [24, 25, 26]

$$\mathbf{Y}_\nu = \begin{pmatrix} \times & 0 \\ 0 & \times \\ \times & 0 \end{pmatrix}, \quad \mathbf{Y}_f = \begin{pmatrix} \times \\ 0 \\ \times \end{pmatrix}, \quad \mathbf{Y}_\ell = \begin{pmatrix} \times & 0 & \times \\ 0 & \times & 0 \\ \times & 0 & \times \end{pmatrix}, \quad \mathbf{M}_R = \begin{pmatrix} 0 & \times \\ \times & \times \end{pmatrix}. \quad (2.8)$$

The simplest symmetry which realises the above patterns and, at the same time, allows CP to be spontaneously broken by the VEV of our complex scalar singlet  $\sigma$  is a  $\mathcal{Z}_8$  Abelian symmetry. In Table 1, we present the field content of our model and respective possible  $\mathcal{Z}_8$  charge assignments. As a matter of fact, there are three possible assignments, labeled as  $\mathcal{Z}_8^{e-\mu}$ ,  $\mathcal{Z}_8^{\mu-\tau}$  and  $\mathcal{Z}_8^{e-\tau}$ , which will lead to the matrices in Eq. (2.8), apart from row and/or column permutations.

In the  $\mathcal{Z}_8^{e-\tau}$  case, the relevant couplings contributing to the mass terms of  $\nu_{1R}$ ,  $\nu_{2R}$  and  $f$  are

$$\frac{1}{2} \frac{1}{\nu_R} \begin{pmatrix} 0 & 0 \\ 0 & (\mathbf{M}_{\text{bare}})_{22} \end{pmatrix} \nu_R^c + \frac{1}{2} \frac{1}{\nu_R} \begin{pmatrix} 0 & (\tilde{\mathbf{Y}}_R)_{12} \\ (\tilde{\mathbf{Y}}_R)_{12} & 0 \end{pmatrix} \nu_R^c \sigma^* + \frac{1}{2} \tilde{y}_f \sigma^* \bar{f} f^c + \text{H.c.}, \quad (2.9)$$

being  $\tilde{\mathbf{Y}}_R$  now a  $2 \times 2$  Yukawa matrix, while  $\tilde{y}_f$  is a complex number.  $\mathbf{M}_{\text{bare}}$  is the  $2 \times 2$  bare RH neutrino mass matrix. This setup allows the complex phase  $\theta$  in  $\langle \sigma \rangle = u e^{i\theta}$  to be successfully transmitted to the effective neutrino mass matrix, giving rise to LCPV.

It is also important to note that just with presence of the scalars  $\Phi$ ,  $\eta$  and  $\sigma$ , the scotogenic radiative correction does not contribute to the effective neutrino mass matrix and consequently, the complex phase of the  $\langle \sigma \rangle$  does not lead to leptonic CP violation. This happens since our  $\mathcal{Z}_8$  symmetry explicitly breaks the term  $(\phi^\dagger \eta)^2$  which closes the loop of Fig. 1. For that reason, we add another dark complex singlet  $\chi$  which transforms oddly under  $\mathcal{Z}_8$  as shown in Table 1. The scalar potential of the model is then given by

$$\begin{aligned} V = & m_\Phi^2 \Phi^\dagger \Phi + m_\eta^2 \eta^\dagger \eta + m_\sigma^2 \sigma^* \sigma + m_\chi^2 \chi^* \chi + \frac{\lambda_1}{2} (\Phi^\dagger \Phi)^2 + \frac{\lambda_2}{2} (\eta^\dagger \eta)^2 + \frac{\lambda_3}{2} (\sigma^* \sigma)^2 + \frac{\lambda_4}{2} (\chi^* \chi)^2 + \lambda_5 (\Phi^\dagger \Phi) (\eta^\dagger \eta) + \\ & + \lambda'_5 (\Phi^\dagger \eta) (\eta^\dagger \Phi) + \lambda_6 (\Phi^\dagger \Phi) (\sigma^* \sigma) + \lambda_7 (\Phi^\dagger \Phi) (\chi^* \chi) + \lambda_8 (\eta^\dagger \eta) (\sigma^* \sigma) + \lambda_9 (\eta^\dagger \eta) (\chi^* \chi) + \lambda_{10} (\sigma^* \sigma) (\chi^* \chi) + \\ & + \left( \frac{\lambda'_3}{4} \sigma^4 + \frac{m_\sigma'^2}{2} \sigma^2 + \mu_1 \chi^2 \sigma + \mu_2 \eta^\dagger \Phi \chi^* + \lambda_{11} \eta^\dagger \Phi \sigma \chi + \text{H.c.} \right), \end{aligned} \quad (2.10)$$

where all parameters are real in order to ensure that the Lagrangian is CP invariant. Note that the term  $m_\sigma'^2 (\sigma^2 + \sigma^{*2})/2$  breaks softly the  $\mathcal{Z}_8$  symmetry, avoiding the formation of cosmological domain walls. Also, radiative neutrino mass generation through the scotogenic loop is allowed by the last three terms of the above potential, as shown in the two diagrams of Fig. 3. After minimizing the scalar potential, one gets the following possible VEV configuration

$$\langle \eta^0 \rangle = 0, \quad \langle \chi \rangle = 0, \quad \langle \phi^0 \rangle = v \quad \text{and} \quad \langle \sigma \rangle = u e^{i\theta}, \quad (2.11)$$

with

$$m_\Phi^2 = -\frac{\lambda_1}{2} v^2 - \frac{\lambda_6}{2} u^2, \quad m_\sigma^2 = -\frac{\lambda_6}{2} v^2 - \frac{\lambda_3 - \lambda'_3}{2} u^2, \quad \cos(2\theta) = -\frac{m_\sigma'^2}{u^2 \lambda'_3}. \quad (2.12)$$

	Fields	SU(2) <sub>L</sub> ⊗ U(1) <sub>Y</sub>	$\mathcal{Z}_8^{e-\mu} \rightarrow \mathcal{Z}_2$	$\mathcal{Z}_8^{\mu-\tau} \rightarrow \mathcal{Z}_2$	$\mathcal{Z}_8^{e-\tau} \rightarrow \mathcal{Z}_2$
Fermions	$L_e, e_R$	(2, -1/2), (1, 0)	$\omega^6 \equiv -i \rightarrow +1$	$\omega^0 \equiv 1 \rightarrow +1$	$\omega^6 \equiv -i \rightarrow +1$
	$L_\mu, \mu_R$	(2, -1/2), (1, 0)	$\omega^6 \equiv -i \rightarrow +1$	$\omega^6 \equiv -i \rightarrow +1$	$\omega^0 \equiv 1 \rightarrow +1$
	$L_\tau, \tau_R$	(2, -1/2), (1, 0)	$\omega^0 \equiv 1 \rightarrow +1$	$\omega^6 \equiv -i \rightarrow +1$	$\omega^6 \equiv -i \rightarrow +1$
	$\nu_R^1$	(1, 0)	$\omega^6 \equiv -i \rightarrow +1$	$\omega^6 \equiv -i \rightarrow +1$	$\omega^6 \equiv -i \rightarrow +1$
	$\nu_R^2$	(1, 0)	$\omega^0 \equiv 1 \rightarrow +1$	$\omega^0 \equiv 1 \rightarrow +1$	$\omega^0 \equiv 1 \rightarrow +1$
	$f$	(1, 0)	$\omega^3 \rightarrow -1$	$\omega^3 \rightarrow -1$	$\omega^3 \rightarrow -1$
Scalars	$\Phi$	(2, 1/2)	$\omega^0 \equiv 1 \rightarrow +1$	$\omega^0 \equiv 1 \rightarrow +1$	$\omega^0 \equiv 1 \rightarrow +1$
	$\sigma$	(1, 0)	$\omega^2 \equiv i \rightarrow +1$	$\omega^2 \equiv i \rightarrow +1$	$\omega^2 \equiv i \rightarrow +1$
	$\eta$	(2, 1/2)	$\omega^5 \rightarrow -1$	$\omega^5 \rightarrow -1$	$\omega^5 \rightarrow -1$
	$\chi$	(1, 0)	$\omega^3 \rightarrow -1$	$\omega^3 \rightarrow -1$	$\omega^3 \rightarrow -1$

TABLE 1: Matter content and charge assignments of the model. Here  $\omega^a = e^{2i\pi a/8}$  is the  $a$ -th power of the eighth root of unity that defines the  $\mathcal{Z}_8$  symmetry.

This solution corresponds to the deepest minimum provided that the condition  $(m_\sigma^4 - u^4 \lambda_3^2)/(4\lambda_3^4) > 0$  is satisfied.

For the present model, one can write an effective neutrino mass matrix analogous to the one given in Eq. (2.2) as

$$\mathbf{M}_\nu = -v^2 \mathbf{Y}_\nu \mathbf{M}_R^{-1} \mathbf{Y}_\nu^T + \mathcal{F}(M_f, m_{S_i}) M_f \mathbf{Y}_f \mathbf{Y}_f^T, \quad (2.13)$$

being  $\mathbf{Y}_\nu$  ( $\mathbf{Y}_f$ ) the Dirac neutrino Yukawa coupling matrix (Yukawa-type coupling matrix of the leptons to the dark fields  $f$  and  $\eta$ ),  $\mathbf{M}_R$  the RH neutrino mass matrix and  $M_f$  the dark fermion  $f$  mass. Like in Eq. (2.2), the first term in Eq. (2.13) corresponds to the seesaw contribution, while the second term accounts for the radiative corrections from the scotogenic contribution. The loop factor  $\mathcal{F}(M_f, m_{S_i})$  depends on the masses  $m_{S_i}$  of the dark scalar mass eigenstates  $S_i$  resulting from the mixing of the neutral components of  $\eta$  and  $\chi$ .

Henceforward, we will consider the  $\mathcal{Z}_8^{e-\tau}$  charge assignment of Table 1, for definiteness. In this case, the following mass and Yukawa matrices are obtained

$$\mathbf{Y}_\nu = \begin{pmatrix} x_1 & 0 \\ 0 & x_2 \\ x_3 & 0 \end{pmatrix}, \quad \mathbf{M}_R = \begin{pmatrix} 0 & M_{12} e^{-i\theta} \\ M_{12} e^{-i\theta} & M_{22} \end{pmatrix}, \quad \mathbf{Y}_f = \begin{pmatrix} y_1 \\ 0 \\ y_2 \end{pmatrix}, \quad \mathbf{Y}_\ell = \begin{pmatrix} w_1 & 0 & w_2 \\ 0 & w_3 & 0 \\ w_4 & 0 & w_5 \end{pmatrix}, \quad (2.14)$$

being  $M_{12} = u (\tilde{\mathbf{Y}}_R)_{12}$  and  $M_{22} = (\mathbf{M}_{\text{bare}})_{22}$ , by comparison with Eq. (2.9). Additionally, the  $f$  mass term is given by  $M_f e^{-i\theta}$  with  $M_f = u \tilde{y}_f$ . The parameters  $M_{12}$ ,  $M_{22}$ ,  $x_i$ ,  $y_i$  and  $w_i$  are real since we imposed CP invariance at the Lagrangian level. The  $\mathbf{Y}_\ell$  texture that arises from  $\mathcal{Z}_8$  invariance results in a decoupled charged-lepton in the symmetry basis. Hence, the charged-lepton contribution to the final lepton mixing is non-trivial. In fact, the charged-lepton mixing matrix is parametrised by a single angle  $\theta_\ell$  as

$$\mathbf{U}_\ell = \begin{pmatrix} \cos \theta_\ell & 0 & \sin \theta_\ell \\ 0 & 1 & 0 \\ -\sin \theta_\ell & 0 & \cos \theta_\ell \end{pmatrix} \mathbf{P}_{ij}, \quad (2.15)$$

being the permutation matrices  $\mathbf{P}_{ij} = \mathbf{P}_{12}$ ,  $\mathbf{1}$  or  $\mathbf{P}_{23}$ , if the considered decoupled charged lepton is the electron ( $\mathcal{Z}_8^{\mu-\tau}$  symmetry), muon ( $\mathcal{Z}_8^{e-\tau}$  symmetry) or tau ( $\mathcal{Z}_8^{e-\mu}$  symmetry), respectively. The permutation matrices are given by

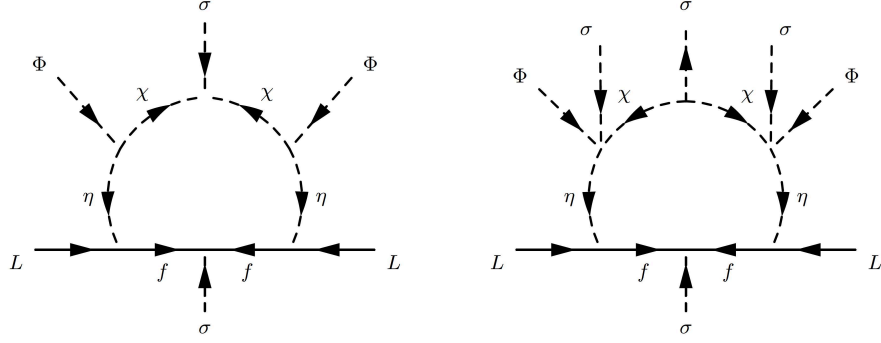
$$\mathbf{P}_{12} = \begin{pmatrix} 0 & 1 & 0 \\ 1 & 0 & 0 \\ 0 & 0 & 1 \end{pmatrix}, \quad \mathbf{P}_{23} = \begin{pmatrix} 1 & 0 & 0 \\ 0 & 0 & 1 \\ 0 & 1 & 0 \end{pmatrix}, \quad (2.16)$$

and  $\mathbf{1}$  is the  $3 \times 3$  identity matrix. Thus, in the charged-lepton physical basis, the charged-lepton and effective neutrino mass matrices are

$$\mathbf{M}'_\ell = \text{diag}(m_e, m_\mu, m_\tau) \quad \text{and} \quad \mathbf{M}'_\nu = \mathbf{U}_\ell^T \mathbf{M}_\nu \mathbf{U}_\ell, \quad (2.17)$$

respectively. Here,  $\mathbf{U}_\ell$  and  $\mathbf{M}_\nu$  are given in Eqs. (2.15) and (2.13), respectively. From Eqs. (2.13) and (2.14), the effective neutrino mass matrix in the original symmetry basis reads

$$\mathbf{M}_\nu = \begin{pmatrix} \mathcal{F}(M_f, m_{S_i}) M_f y_1^2 + \frac{v^2 M_{22}}{M_{12}^2} x_1^2 e^{i\theta} & -\frac{v^2}{M_{12}} x_1 x_2 & \mathcal{F}(M_f, m_{S_i}) M_f y_1 y_2 + \frac{v^2 M_{22}}{M_{12}^2} x_1 x_3 e^{i\theta} \\ \cdot & 0 & -\frac{v^2}{M_{12}} x_2 x_3 \\ \cdot & \cdot & \mathcal{F}(M_f, m_{S_i}) M_f y_2^2 + \frac{v^2 M_{22}}{M_{12}^2} x_3^2 e^{i\theta} \end{pmatrix}. \quad (2.18)$$

FIGURE 3: One-loop diagrams contributing to neutrino mass generation in the minimal  $Z_8$  scoto-seesaw model.

Parameter	Best Fit $\pm 1\sigma$	$3\sigma$ range
$\theta_{12}$ ( $^\circ$ ) [NO] [IO]	$34.3 \pm 1.0$	$31.4 - 37.4$
$\theta_{23}$ ( $^\circ$ ) [NO]	$48.79^{+0.93}_{-1.25}$	$41.63 - 51.32$
$\theta_{23}$ ( $^\circ$ ) [IO]	$48.79^{+1.04}_{-1.30}$	$41.88 - 51.30$
$\theta_{13}$ ( $^\circ$ ) [NO]	$8.58^{+0.11}_{-0.15}$	$8.16 - 8.94$
$\theta_{13}$ ( $^\circ$ ) [IO]	$8.63^{+0.11}_{-0.15}$	$8.21 - 8.99$
$\delta/\pi$ [NO]	$1.20^{+0.23}_{-0.14}$	$0.80 - 2.00$
$\delta/\pi$ [IO]	$1.54 \pm 0.13$	$1.14 - 1.90$
$\Delta m_{21}^2$ ( $\times 10^{-5}$ eV $^2$ ) [NO] [IO]	$7.50^{+0.22}_{-0.20}$	$6.94 - 8.14$
$ \Delta m_{31}^2 $ ( $\times 10^{-3}$ eV $^2$ ) [NO]	$2.56^{+0.03}_{-0.04}$	$2.46 - 2.65$
$ \Delta m_{31}^2 $ ( $\times 10^{-3}$ eV $^2$ ) [IO]	$2.46 \pm 0.03$	$2.37 - 2.55$

TABLE 2: Neutrino oscillation parameters obtained from the global analysis of Ref. [19].

The texture zero  $(\mathbf{M}_\nu)_{22} = 0$  arises directly from the considered  $Z_8^{\ell-\tau}$  symmetry. One can demonstrate that the existence of CP violation is crucially ensured by the contribution of the scotogenic loop. If this contribution vanishes, then the vacuum phase  $\theta$  can be rephased away and CP is conserved. Moreover, due to the fact that there is only a two state mixing in the charged-lepton sector, the zero condition in  $\mathbf{M}_\nu$  translates into

$$(\mathbf{M}'_\nu)_{ii} = 0 \text{ for decoupled } e_i, \quad (2.19)$$

in the charged-lepton mass basis, after performing the  $\mathbf{U}_\ell$  rotation shown in Eq. (2.17). Here,  $i = 1, 2, 3$  for  $e, \mu$  and  $\tau$ , respectively.

### 3. LOW-ENERGY CONSTRAINTS FROM NEUTRINO OSCILLATION DATA

We will proceed with the analysis of the constraints set by the condition in Eq. (2.19) on parameters at low energies. For that we write  $\mathbf{M}'_\nu$  in terms of neutrino masses and lepton mixing angles as

$$\mathbf{M}'_\nu = \mathbf{U}^* \mathbf{d}_m \mathbf{U}^\dagger, \quad \mathbf{d}_m \equiv \text{diag}(m_1, m_2, m_3), \quad (3.1)$$

being  $m_i$  the light neutrino masses and  $\mathbf{U}$  the lepton mixing matrix, which may be symmetrically parametrised as [27]

$$\mathbf{U} = \begin{pmatrix} c_{12}c_{13} & s_{12}c_{13}e^{-i\phi_{12}} & s_{13}e^{-i\phi_{13}} \\ -s_{12}c_{23}e^{i\phi_{12}} - c_{12}s_{13}s_{23}e^{-i(\phi_{23}-\phi_{13})} & c_{12}c_{23} - s_{12}s_{13}s_{23}e^{-i(\phi_{12}+\phi_{23}-\phi_{13})} & c_{13}s_{23}e^{-i\phi_{23}} \\ s_{12}s_{23}e^{i(\phi_{12}+\phi_{23})} - c_{12}s_{13}c_{23}e^{i\phi_{13}} & -c_{12}s_{23}e^{i\phi_{23}} - s_{12}s_{13}c_{23}e^{-i(\phi_{12}-\phi_{13})} & c_{13}c_{23} \end{pmatrix}. \quad (3.2)$$

The matrix  $\mathbf{U}$  is, thus, parametrised by the lepton mixing angles  $\theta_{ij}$  ( $i < j = 1, 2, 3$ ), being  $s_{ij} \equiv \sin \theta_{ij}$  and  $c_{ij} \equiv \cos \theta_{ij}$ , and three phases  $\phi_{13}, \phi_{12}$  and  $\phi_{23}$ . The Dirac phase is given by  $\delta = \phi_{13} - \phi_{12} - \phi_{23}$  and the two Majorana phases are  $\phi_{12,13}$ . One can write two neutrino masses in terms of the two neutrino mass-squared differences  $\Delta m_{21}^2 = m_2^2 - m_1^2$  and  $\Delta m_{31}^2 = m_3^2 - m_1^2$ , measured in oscillation experiments, and the lightest neutrino mass  $m_{\text{lightest}}$  – which corresponds to  $m_1$  for a normally ordered (NO) neutrino

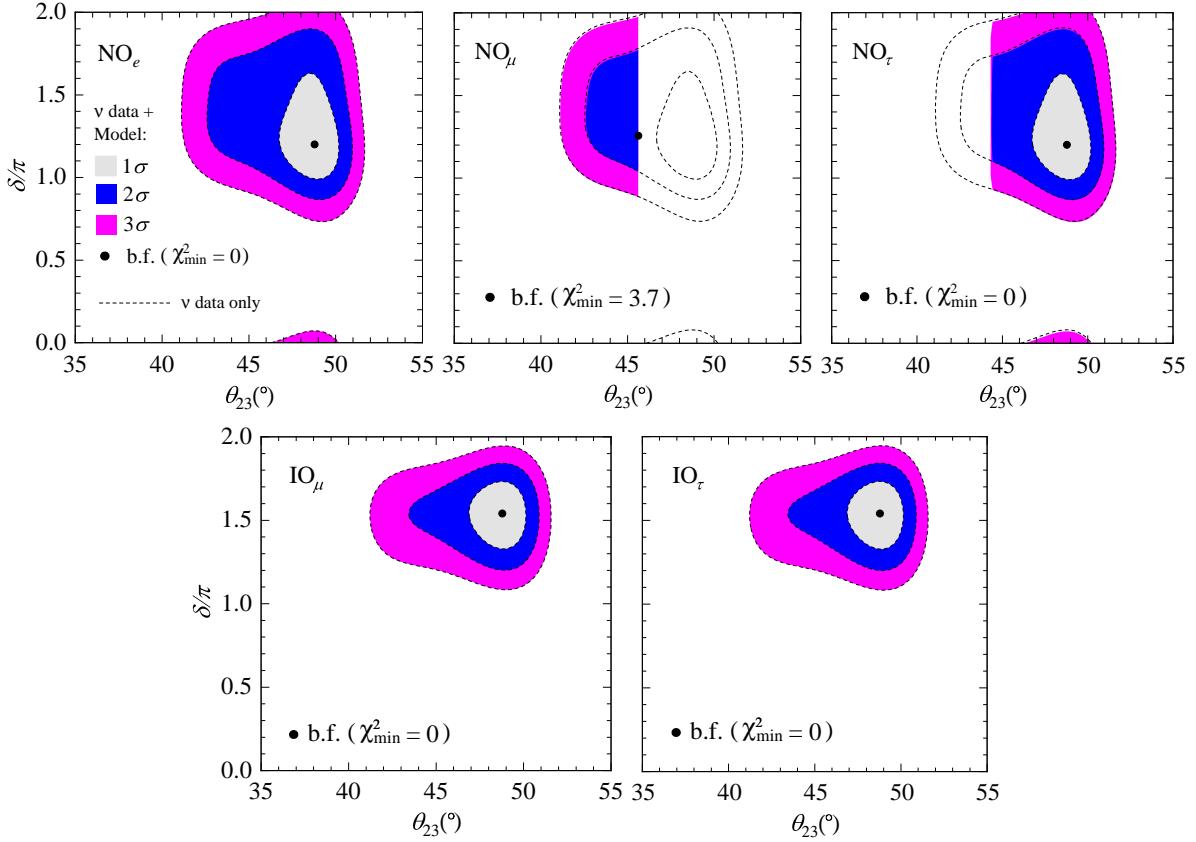


FIGURE 4: Allowed regions in the  $(\theta_{23}, \delta)$  plane for  $NO_{e,\mu,\tau}$  (upper plots) and  $IO_{\mu,\tau}$  (lower plots) for the considered  $Z_8$  model. The dashed lines delimit the viable regions which result from considering only neutrino oscillation data.

mass spectrum and to  $m_3$  for an inverted ordered (IO) neutrino mass spectrum – as

$$\text{NO: } m_2 = \sqrt{m_{\text{lightest}}^2 + \Delta m_{21}^2}, \quad m_3 = \sqrt{m_{\text{lightest}}^2 + \Delta m_{31}^2}, \quad (3.3)$$

$$\text{IO: } m_1 = \sqrt{m_{\text{lightest}}^2 + |\Delta m_{21}^2|}, \quad m_2 = \sqrt{m_{\text{lightest}}^2 + \Delta m_{21}^2 + |\Delta m_{31}^2|}. \quad (3.4)$$

In Table 2, we show the present experimental intervals for the three mixing angles, two neutrino mass-squared differences and the Dirac phase, resulting from the global fit to neutrino oscillation data of Ref. [19].

In Figs. 4 and 5 we show the  $(\theta_{23}, \delta)$  and  $(m_{\text{lightest}}, \delta)$  allowed regions at the  $1\sigma$ ,  $2\sigma$  and  $3\sigma$  levels (in gray, blue and magenta, respectively), for schemes with decoupled  $e$ ,  $\mu$  and  $\tau$ , with both NO (upper panels) and IO (lower panels) neutrino mass spectra. We label these different frameworks as  $NO_{e,\mu,\tau}$  and  $IO_{e,\mu,\tau}$ . In order to calculate the  $\chi^2$  contours, we use the one-dimensional (two-dimensional) global-fit profiles from [19] for  $s_{12}^2, s_{13}^2, \Delta m_{21}^2$  and  $\Delta m_{31}^2$  (for  $\theta_{23}$  and  $\delta$ ). This fitting method is implemented under the constraint given in Eq. (2.19) for any of the three cases to be analysed, corresponding to decoupled  $e$ , muon and tau. Note that we do not combine further constraints on  $m_{\text{lightest}}$  either from cosmology or  $\beta$ -decay experiments. Alternatively, we show in Fig. 5 our results in terms of  $m_{\text{lightest}}$ , indicating the aforementioned bounds by a shaded band and a vertical dashed red line, respectively. The shaded band demarcates the most and less conservative upper limits coming from cosmology. The left (right) delimiting black dotted line represents the Planck TT, TE, EE + lowE + lensing + BAO (Planck TT + lowE) 95% CL limit  $\sum_k m_k < 0.12$  eV (0.54 eV). In turn, the vertical red dashed line delimits the  $m_{\text{lightest}}$  KATRIN tritium beta decay 90% CL upper limit  $m_\beta < 1.1$  eV. Also, in Fig. 4, we show the (dashed) lines which limit the parameter space allowed by data alone (without “prior” model constraints).

Since the relation  $(\mathbf{M}'_V)_{11} = 0$  corresponds to a vanishing rate for  $0\nu\beta\beta$  decay, the case  $IO_e$  is not compatible with data. Furthermore, by inspecting the leftmost upper panel of Fig. 4, we conclude that the  $NO_e$  model-allowed regions in the  $(\theta_{23}, \delta)$  plane correspond to the data allowed ones obtained in [19]. This happens since  $(\mathbf{M}'_V)_{11}$  does not have any dependence on  $\delta$  and  $\theta_{23}$ . On the other hand, from the middle (right-handed) upper plot of Fig. 4 one concludes that the  $NO_\mu$  ( $NO_\tau$ ) case shows a preference for the first (second)  $\theta_{23}$  octant. Hence,  $NO_\tau$  is consistent with data at  $1\sigma$ , while  $NO_\mu$  is only compatible at the  $2\sigma$  level. Interestingly, future experiments like T2HK will most probably be able to untangle the  $\theta_{23}$  octant ambiguity and consequently, exclude either the  $NO_\mu$  or the  $NO_\tau$  case. In what concerns the cases  $IO_{\mu,\tau}$ , from the lower panels in Fig. 4, one can see again that the  $(\theta_{23}, \delta)$  regions coincide with the ones allowed by the present global fits.

Although the  $(\theta_{23}, \delta)$  compatibility regions coincide with experimental ones for the cases  $NO_e$ ,  $IO_\mu$  and  $IO_\tau$ , these are only viable for a specific range of  $m_{\text{lightest}}$ , as shown in Fig. 5. In particular, for the case  $NO_e$  to be compatible with data,  $m_{\text{lightest}}$  has to

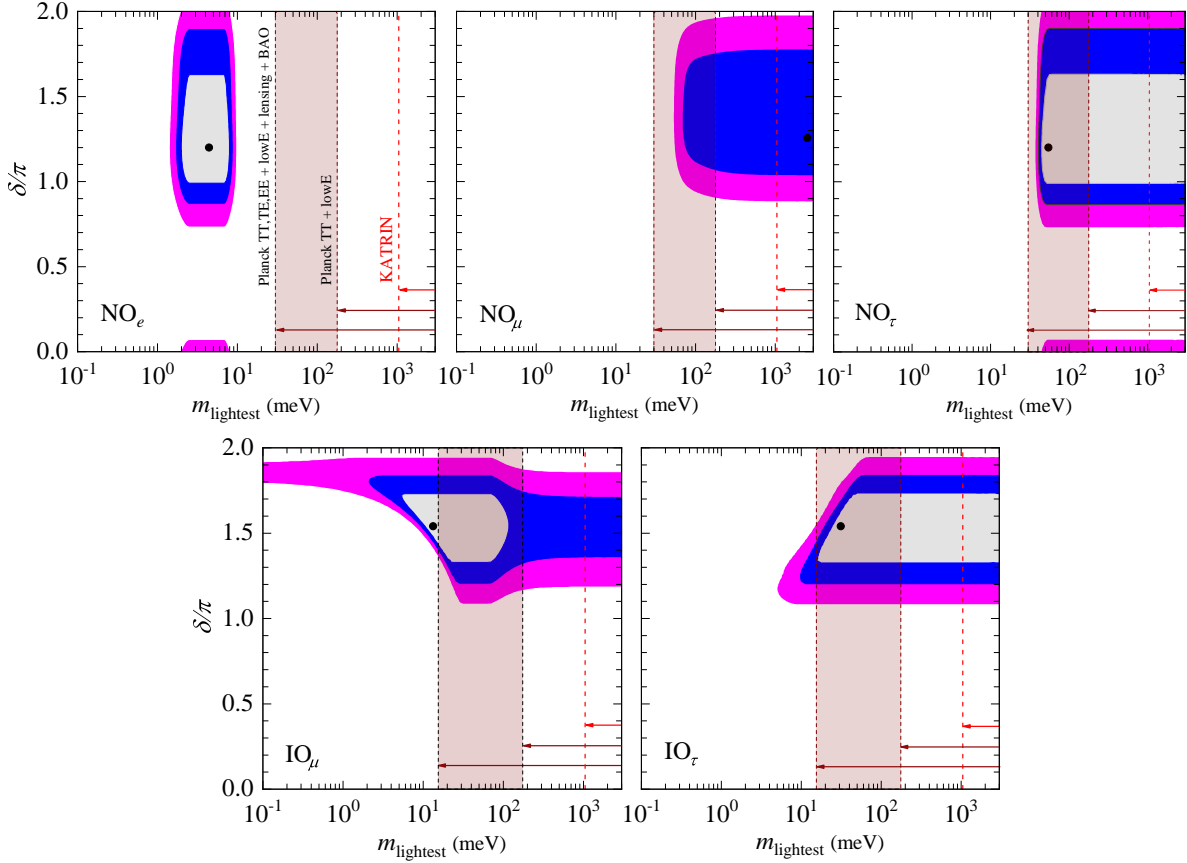


FIGURE 5: Allowed regions in the  $(m_{\text{lightest}}, \delta)$  plane for NO (upper plots) and IO (lower plots) for the considered  $\mathcal{Z}_8$  model. For the color code of the allowed regions see Fig. 4. The vertical red dashed line corresponds to the  $m_{\text{lightest}}$  KATRIN upper limit  $m_\beta < 1.1$  eV (90% CL). The vertical shaded band shows the upper-limit range for  $m_{\text{lightest}}$  from  $\sum_k m_k$  cosmological bounds.

be in the range [20, 80] meV, at the  $3\sigma$  level. This corresponds to an upper and a lower bound on  $m_{\text{lightest}}$ , both of them below those following from current beta decay experiments and cosmology. In Fig. 5, these bounds are delimited, respectively, by a red dashed line and a vertical shaded band. Regarding the case  $\text{IO}_\mu$ , the allowed  $m_{\text{lightest}}$  interval at  $1\sigma$  corresponds to [5, 100] meV. In turn, for  $\text{IO}_\tau$ , a 16 meV lower bound at the  $1\sigma$  level can be identified, lying closely to the most stringent cosmological limit.

#### 4. PREDICTIONS FOR NEUTRINOLESS DOUBLE BETA DECAY

Taking into account the presented results for the lightest neutrino mass and the neutrino oscillation parameters, we now show the model allowed parameter space for the effective mass  $m_{\beta\beta}$ , which characterizes the probability of observing neutrinoless double beta decays. The exchange of light neutrinos contributes to  $m_{\beta\beta}$  as

$$\text{NO} : m_{\beta\beta} = \left| c_{12}^2 c_{13}^2 m_{\text{lightest}} + s_{12}^2 c_{13}^2 \sqrt{m_{\text{lightest}}^2 + \Delta m_{21}^2} e^{2i\phi_{12}} + s_{13}^2 \sqrt{m_{\text{lightest}}^2 + \Delta m_{31}^2} e^{2i\phi_{13}} \right|, \quad (4.1)$$

$$\text{IO} : m_{\beta\beta} = \left| c_{12}^2 c_{13}^2 \sqrt{m_{\text{lightest}}^2 + \Delta m_{21}^2} + s_{12}^2 c_{13}^2 \sqrt{m_{\text{lightest}}^2 + \Delta m_{21}^2} + |\Delta m_{31}^2| e^{2i\phi_{12}} + s_{13}^2 m_{\text{lightest}} e^{2i\phi_{13}} \right|, \quad (4.2)$$

in the symmetrical parametrisation of  $\mathbf{U}$  [21, 27], for the cases of NO and IO, respectively.

In Fig. 6, we present the predictions for  $m_{\beta\beta}$  taking into account the constraints given in Eq. (2.19) and the global-fit analysis from Ref. [19]. The results are shown in the plane  $(m_{\text{lightest}}, m_{\beta\beta})$ , and are complementary to those in Figs. 4 and 5. As before, the NO (IO) cases are presented in the upper (lower) panels of Fig. 6. We indicate as well the current upper bounds from  $0\nu\beta\beta$  searches at EXO-200 [28], CUORE [29], GERDA [30] and KamLAND-Zen 400 [31]. Notice that  $m_{\beta\beta} = 0$  is predicted by the case  $\text{NO}_e$  and, thus, is not shown. From the allowed regions presented in Fig. 6, it can be seen that, even for NO, the model imposes a lower bound on  $m_{\beta\beta}$ . It is interesting to note that this feature holds even with the presence of a simple  $\mathcal{Z}_8$  symmetry. Indeed, it can be seen that the present  $m_{\beta\beta}$  KamLAND bound is on the verge of excluding the  $\text{NO}_{\mu,\tau}$  cases. Data from forthcoming experiments such as KamLAND2-Zen [31], CUPID [32], SNO+ I [33], PandaX-III [34], nEXO [35], LEGEND [36], or AMORE II [37] should be able to probe the entirety of the model allowed regions. In what concerns the IO cases, the allowed regions by neutrino oscillation data are

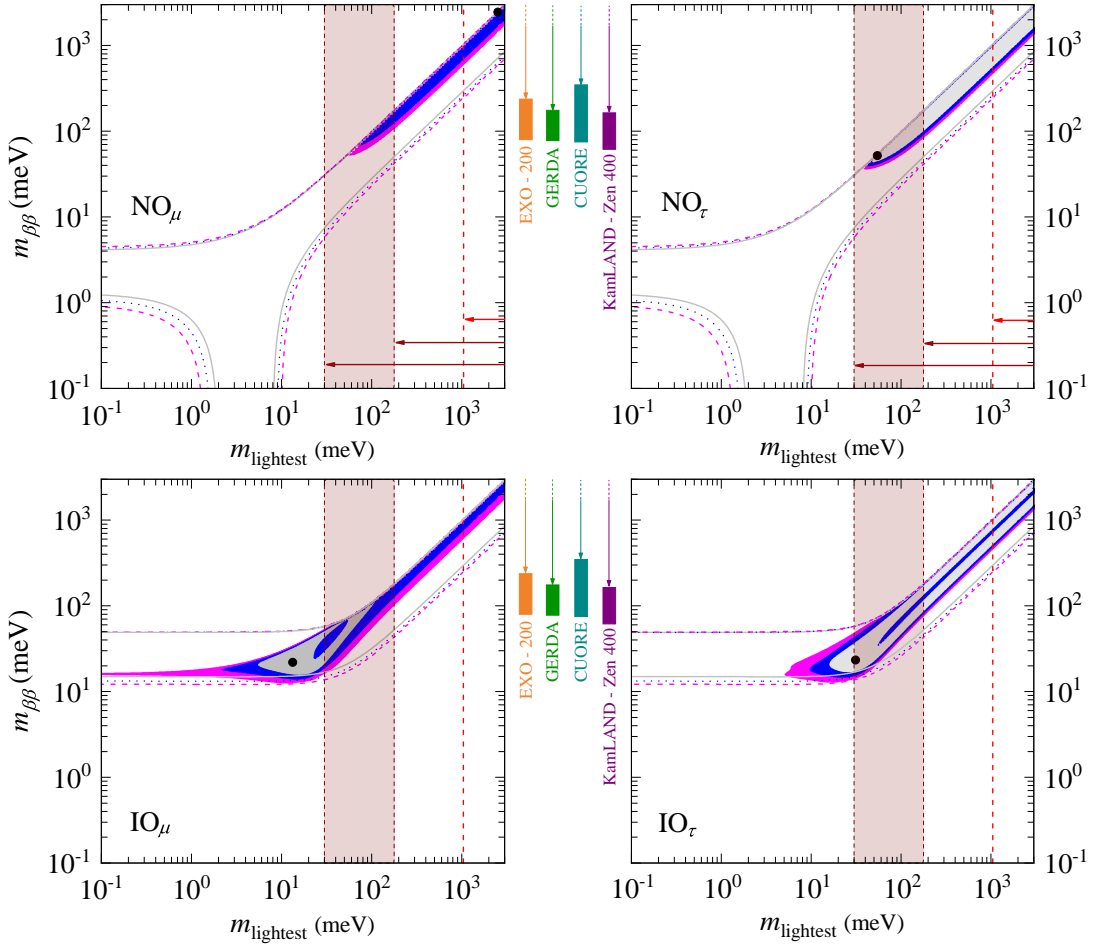


FIGURE 6: Allowed regions in the  $(m_{\text{lightest}}, m_{\beta\beta})$  plane for NO (upper panels) and IO (lower panels). For the color code of the allowed regions see Fig. 4. The solid (dotted) [dashed] lines delimit the  $1\sigma$  ( $2\sigma$ ) [ $3\sigma$ ]  $m_{\beta\beta}$  regions allowed in the general unconstrained case. The vertical bars placed in between the panels indicate the present  $m_{\beta\beta}$  upper bounds from EXO-200 [28], CUORE [29], GERDA [30] and KamLAND-Zen 400 [31] at 95%CL. The height of the bars corresponds to the ambiguity in the nuclear matrix elements, important for decay rate computation.

also already being scrutinized by current upper bounds on  $m_{\beta\beta}$ . Still, expected sensitivities from next-generation experiments will be able to thoroughly probe the IO allowed regions.

## 5. CONCLUSIONS

We have introduced a simple scoto-seesaw model with an underlying  $\mathcal{Z}_8$  symmetry, where neutrino masses are generated at tree level via type-I seesaw mechanism, and at radiative level through a scotogenic loop. In this case, spontaneous CP violation and DM stability arise from the  $\mathcal{Z}_8$  breaking to a dark  $\mathcal{Z}_2$  by the complex VEV of a scalar singlet  $\sigma$ . The complex VEV of  $\sigma$  constitutes the only source of CP violation, which is successfully transmitted to the neutrino sector through the  $\sigma/\sigma^*$  couplings to the RH neutrinos  $\nu_R$  and the dark fermion  $f$ . Moreover, the  $\mathcal{Z}_8$  flavour symmetry imposes low-energy constraints that were tested against neutrino oscillation data. The obtained results are given in Figs. 4, 5 and 6, for both normal and inverted ordering neutrino mass spectra. As can be seen in Fig. 6, for normal ordering, the obtained lightest-neutrino mass ranges will be completely probed by upcoming neutrinoless double beta decay searches and by enhanced sensitivities on neutrino masses in cosmological searches (with the exception of the case that predicts  $m_{\beta\beta} = 0$ ). On the other hand, for inverted ordering, we conclude that an improved measurement of the Dirac phase is needed in order to test our model.

This model was build with the intention of providing a template for a dynamical origin of leptonic CP violation, rather than proposing just another model for DM and neutrino masses. This was accomplished by connecting an answer to the DM problem with neutrino masses through CP violation, induced by the same scalar singlet which gives mass to the fermion that mediates light-neutrino mass generation.

Let us conclude by discussing the dark sector of our model. The first aspect we may notice is that our dark sector is enlarged when comparing to that of the canonical model, due to the presence of an extra scalar singlet  $\chi$ . Just like in other scotogenic-type

extensions of the SM [2, 3, 4, 5, 6, 7, 8, 9, 10, 11, 12, 13], in our case also the lightest dark-sector particle is stabilized by the presence of a remnant  $Z_2$  subgroup after breaking of the flavour  $Z_8$  group, as seen in Table 1. Thus, the lightest of the dark particles, being it a fermion or a scalar, is an adequate DM candidate. The presence of the new scalar singlet  $\sigma$  allows for the new dark scalar  $\chi$  to mix with the usual dark scalar  $\eta$ . Consequently, this model will have an enlarged compatible parameter space with the observed DM relic density, when comparing with the canonical scotogenic model [2]. As a matter of fact, the addition of a dark scalar singlet, as for instance  $\chi$  in our case, has been shown to largely increase the parameter space of the model [38]. Furthermore, the inclusion of a scalar with non-zero VEV, e.g.  $\sigma$  in our model, also enhances the viability range, in the case where DM is the lightest Majorana fermion [39]. Our model has both of these two features and, thus, its allowed parameter space will be certainly larger than those of the simplest scotogenic model and the above extensions. Any expected DM signature, will thus be comparable to those discussed in the above-mentioned scotogenic extensions.

## ACKNOWLEDGMENTS

This work is supported by the Spanish grants SEV-2014-0398 and FPA2017-85216-P (AEI/FEDER, UE), PROMETEO/2018/165 (Generalitat Valenciana), the Spanish Red Consolider MultiDark FPA2017-90566-REDC and Fundação para a Ciência e a Tecnologia (FCT, Portugal) through the projects UIDB/00777/2020, UIDP/00777/2020, CERN/FIS-PAR/0004/2019, and PTDC/FIS-PAR/29436/2017. D.M.B. is supported by the FCT grant SFRH/BD/137127/2018. R.S. is supported by SERB, Government of India grant SRG/2020/002303.

## References

- [1] D. M. Barreiros, F. R. Joaquim, R. Srivastava and J. W. F. Valle, “Minimal scoto-seesaw mechanism with spontaneous CP violation,” *JHEP* (2021) 249, arXiv:2012.05189 [hep-ph].
- [2] E. Ma, “Verifiable radiative seesaw mechanism of neutrino mass and dark matter,” *Phys.Rev.* **D73** (2006) 077301.
- [3] E. Ma and D. Suematsu, “Fermion Triplet Dark Matter and Radiative Neutrino Mass,” *Mod.Phys.Lett.* **A24** (2009) 583–589, arXiv:0809.0942 [hep-ph].
- [4] M. Hirsch *et al.*, “WIMP dark matter as radiative neutrino mass messenger,” *JHEP* **1310** (2013) 149, arXiv:1307.8134 [hep-ph].
- [5] A. Merle *et al.*, “Consistency of WIMP Dark Matter as radiative neutrino mass messenger,” *JHEP* **1607** (2016) 013, arXiv:1603.05685 [hep-ph].
- [6] M. A. Díaz *et al.*, “Heavy Higgs Boson Production at Colliders in the Singlet-Triplet Scotogenic Dark Matter Model,” *JHEP* **1708** (2017) 017, arXiv:1612.06569 [hep-ph].
- [7] S. Choubey, S. Khan, M. Mitra, and S. Mondal, “Singlet-Triplet Fermionic Dark Matter and LHC Phenomenology,” *Eur.Phys.J.* **C78** (2018) 302, arXiv:1711.08888 [hep-ph].
- [8] C. Bonilla, S. Centelles-Chuliá, R. Cepedello, E. Peinado, and R. Srivastava, “Dark matter stability and Dirac neutrinos using only Standard Model symmetries,” *Phys. Rev. D* **101** no. 3, (2020) 033011, arXiv:1812.01599 [hep-ph].
- [9] S. Centelles Chuliá, R. Cepedello, E. Peinado, and R. Srivastava, “Scotogenic dark symmetry as a residual subgroup of Standard Model symmetries,” *Chin. Phys. C* **44** no. 8, (2020) 083110, arXiv:1901.06402 [hep-ph].
- [10] C. Bonilla, E. Peinado, and R. Srivastava, “The role of residual symmetries in dark matter stability and the neutrino nature,” *LHEP* **2** no. 1, (2019) 124, arXiv:1903.01477 [hep-ph].
- [11] S. Centelles Chuliá, R. Cepedello, E. Peinado, and R. Srivastava, “Systematic classification of two loop  $d = 4$  Dirac neutrino mass models and the Diracness-dark matter stability connection,” *JHEP* **10** (2019) 093, arXiv:1907.08630 [hep-ph].
- [12] D. Restrepo and A. Rivera, “Phenomenological consistency of the singlet-triplet scotogenic model,” *JHEP* **2004** (2020) 134, arXiv:1907.11938 [hep-ph].
- [13] I. M. Ávila, V. De Romeri, L. Duarte, and J. W. Valle, “Minimalistic scotogenic scalar dark matter,” arXiv:1910.08422 [hep-ph].
- [14] S. K. Kang, O. Popov, R. Srivastava, J. W. Valle, and C. A. Vaquera-Araujo, “Scotogenic dark matter stability from gauged matter parity,” *Phys.Lett.* **B798** (2019) 135013, arXiv:1902.05966 [hep-ph].
- [15] J. Leite, O. Popov, R. Srivastava, and J. W. Valle, “A theory for scotogenic dark matter stabilised by residual gauge symmetry,” arXiv:1909.06386 [hep-ph].
- [16] A. Cárcamo Hernández, J. W. Valle, and C. A. Vaquera-Araujo, “Simple theory for scotogenic dark matter with residual matter-parity,” arXiv:2006.06009 [hep-ph].
- [17] J. Leite, A. Morales, J. W. Valle, and C. A. Vaquera-Araujo, “Dark matter stability from Dirac neutrinos in scotogenic 3-3-1-1 theory,” arXiv:2005.03600 [hep-ph].
- [18] J. Leite, A. Morales, J. W. Valle, and C. A. Vaquera-Araujo, “Scotogenic dark matter and Dirac neutrinos from unbroken gauged  $B - L$  symmetry,” arXiv:2003.02950 [hep-ph].
- [19] P. F. de Salas, D. V. Forero, S. Gariazzo, P. Martínez-Miravé, O. Mena, C. A. Ternes, M. Tórtola and J. W. F. Valle, “2020 global reassessment of the neutrino oscillation picture,” *JHEP* **02** (2021), 071 arXiv:2006.11237 [hep-ph].
- [20] N. Rojas, R. Srivastava, and J. W. F. Valle, “Simplest Scoto-Seesaw Mechanism,” *Phys.Lett.* **B789** (2019) 132–136, arXiv:1807.11447 [hep-ph].
- [21] J. Schechter and J. W. F. Valle, “Neutrino Masses in  $SU(2) \times U(1)$  Theories,” *Phys.Rev.* **D22** (1980) 2227.
- [22] G. C. Branco, L. Lavoura, and J. P. Silva, “CP Violation,” *Int.Ser.Monogr.Phys.* **103** (1999) 1–536.
- [23] G. Branco, R. Felipe, and F. Joaquim, “Leptonic CP Violation,” *Rev. Mod. Phys.* **84** (2012) 515–565, arXiv:1111.5332 [hep-ph].
- [24] D. Barreiros, R. Felipe, and F. Joaquim, “Minimal type-I seesaw model with maximally restricted texture zeros,” *Phys. Rev. D* **97** no. 11, (2018) 115016, arXiv:1802.04563 [hep-ph].
- [25] D. Barreiros, R. Felipe, and F. Joaquim, “Combining texture zeros with a remnant CP symmetry in the minimal type-I seesaw,” *JHEP* **01** (2019) 223, arXiv:1810.05454 [hep-ph].
- [26] D. Barreiros, F. Joaquim, and T. Yanagida, “New approach to neutrino masses and leptogenesis with Occam’s razor,” *Phys. Rev. D* **102** no. 5, (2020) 055021, arXiv:2003.06332 [hep-ph].

- [27] W. Rodejohann and J. W. F. Valle, "Symmetrical Parametrizations of the Lepton Mixing Matrix," *Phys. Rev. D* **84** (2011) 073011, [arXiv:1108.3484 \[hep-ph\]](#).
- [28] **EXO-200** Collaboration, G. Anton *et al.*, "Search for Neutrinoless Double- $\beta$  Decay with the Complete EXO-200 Dataset," *Phys. Rev. Lett.* **123** no. 16, (2019) 161802, [arXiv:1906.02723 \[hep-ex\]](#).
- [29] **CUORE** Collaboration, D. Adams *et al.*, "Improved Limit on Neutrinoless Double-Beta Decay in  $^{130}\text{Te}$  with CUORE," *Phys. Rev. Lett.* **124** no. 12, (2020) 122501, [arXiv:1912.10966 \[nucl-ex\]](#).
- [30] **GERDA** Collaboration, M. Agostini *et al.*, "Final Results of GERDA on the Search for Neutrinoless Double- $\beta$  Decay," [arXiv:2009.06079 \[nucl-ex\]](#).
- [31] **KamLAND-Zen** Collaboration, A. Gando *et al.*, "Search for Majorana Neutrinos near the Inverted Mass Hierarchy Region with KamLAND-Zen," *Phys. Rev. Lett.* **117** no. 8, (2016) 082503, [arXiv:1605.02889 \[hep-ex\]](#). [Addendum: *Phys.Rev.Lett.* **117**, 109903 (2016)].
- [32] **CUPID** Collaboration, G. Wang *et al.*, "CUPID: CUORE (Cryogenic Underground Observatory for Rare Events) Upgrade with Particle Identification," [arXiv:1504.03599 \[physics.ins-det\]](#).
- [33] **SNO+** Collaboration, S. Andringa *et al.*, "Current Status and Future Prospects of the SNO+ Experiment," *Adv. High Energy Phys.* **2016** (2016) 6194250, [arXiv:1508.05759 \[physics.ins-det\]](#).
- [34] X. Chen *et al.*, "PandaX-III: Searching for neutrinoless double beta decay with high pressure  $^{136}\text{Xe}$  gas time projection chambers," *Sci. China Phys. Mech. Astron.* **60** no. 6, (2017) 061011, [arXiv:1610.08883 \[physics.ins-det\]](#).
- [35] **nEXO** Collaboration, J. Albert *et al.*, "Sensitivity and Discovery Potential of nEXO to Neutrinoless Double Beta Decay," *Phys. Rev. C* **97** no. 6, (2018) 065503, [arXiv:1710.05075 \[nucl-ex\]](#).
- [36] **LEGEND** Collaboration, N. Abgrall *et al.*, "The Large Enriched Germanium Experiment for Neutrinoless Double Beta Decay (LEGEND)," vol. 1894, p. 020027. 2017. [arXiv:1709.01980 \[physics.ins-det\]](#).
- [37] **AMoRE** Collaboration, M. H. Lee, "AMoRE: A search for neutrinoless double-beta decay of  $^{100}\text{Mo}$  using low-temperature molybdenum-containing crystal detectors," *JINST* **15** no. 08, (2020) C08010, [arXiv:2005.05567 \[physics.ins-det\]](#).
- [38] A. Beniwal, J. Herrero-García, N. Leerdam, M. White, and A. G. Williams, "The ScotoSinglet Model: A Scalar Singlet Extension of the Scotogenic Model," [arXiv:2010.05937 \[hep-ph\]](#).
- [39] C. Bonilla, L. M. de la Vega, J. Lamprea, R. A. Lineros, and E. Peinado, "Fermion Dark Matter and Radiative Neutrino Masses from Spontaneous Lepton Number Breaking," *New J.Phys.* **22** (2020) 033009, [arXiv:1908.04276 \[hep-ph\]](#).